ROYAL SOCIETY
OF CHEMISTRY

PAPER

Check for updates

Synthesis and electrochromic properties of polyamines containing a 4,4'-diaminotriphenyl-amine-*N,N'*-diyl unit in the polymer backbone: Ru-catalyzed N−H insertion polycondensation of 1,4-phenylenebis(diazoacetate) with 4,4'-diaminotriphenylamine derivatives†

Yun-Chi Wang,[a] Yu-Jen Shao,[a] Guey-Sheng Liou, ORCID *[a] Sota Nagao,[b] Yusuke Makino,[b] Eita Akiyama,[b] Masaaki Kato,[b] Hiroaki Shimomoto ORCID *[b] and Eiji Ihara ORCID *[b]

A new type of polyamine containing a 4,4'-diaminotriphenylamine-*N,N'*-diyl unit in the main chain was prepared by Ru-catalyzed polycondensation of a bis(diazocarbonyl) compound with 4,4'-diaminotri-phenylamine, where the propagation is N−H insertion of a carbene−carbon atom generated from the diazocarbonyl group of the former monomer with N_2 elimination. In the well-defined polyamines newly prepared in this study, the two primary amino groups in the diamine monomer remain as secondary amino groups in the polymer main chain, in contrast to the previously reported polymers prepared by polycondensation of the same diamine monomers, where the amino groups were incorporated into an amide or imide linkage. The resulting triphenyl amino framework in the polymer main chain possesses three amino groups, each of which can independently participate in the electrochemical process as a redox center with applied electrochemical potentials. The electrochromic properties of thin films and electrochromic devices of the polyamines were evaluated with cyclic voltammetry and spectroelectrochemistry, revealing that the polyamines indeed underwent an expected three-stage redox process.

Introduction

In the last two decades, polymerization of diazocarbonyl compounds has been intensively investigated, because the unique reactivity of a diazocarbonyl group can afford a variety of polymer structures that cannot be obtained by any other types of polymerization. For example, C1 polymerization of diazoacetates has been recognized as a useful method for C–C main chain polymer synthesis, which can yield polymers bearing an alkoxycarbonyl group (ester) on each main chain

carbon atom.[1–6] Recent progress has demonstrated that C1 polymerization can yield C–C polymers with a high M_n in good yields, even stereospecifically or in a controlled manner by a suitable choice of a transition metal-based initiator.[7–17]

Along with the above-mentioned C1 polymerization, the use of bis(diazocarbonyl) compounds as a monomer for polycondensation has also been explored and demonstrated to be effective for preparing polymers with a variety of unprecedented main chain structures.[18–31] One of the examples of the polycondensation of bis(diazocarbonyl) compounds utilizes insertion of diazo-bearing carbon atoms into N–H bonds of diamine monomers, affording a variety of polyamines with unique polymer backbone structures. Indeed, the polymerization proceeded efficiently between diethyl 1,4-phenylenebis(diazoacetate) **1** and a variety of aromatic diamines, yielding polyamines bearing an alkoxycarbonyl group at the adjacent carbon of each nitrogen in the main chain framework as shown in Scheme 1.[23] Then, it occurred to us that if we choose 4,4'-diaminotriphenylamine (diamino-TPA) derivatives **2a** and

[a]Institute of Polymer Science and Engineering, National Taiwan University, Taipei 10617, Taiwan. E-mail: gsliou@ntu.edu.tw; Tel: +886-2-33665315
[b]Department of Materials Science and Biotechnology, Graduate School of Science and Engineering, Ehime University, 3 Bunkyo-cho, Matsuyama 790-8577, Japan. E-mail: shimomoto.hiroaki.mx@ehime-u.ac.jp, ihara@ehime-u.ac.jp; Fax: +81-89-927-9949, +81-89-927-8547; Tel: +81-89-927-9949, +81-89-927-8547
†Electronic supplementary information (ESI) available: Experimental procedure, NMR spectra of **P3-OMe**, SEC charts of **P3**s, FT-IR spectra of **P3**s, TGA and DSC thermograms of **P3**s, and photographs of **P3**s during cyclic voltammetry analyses. See DOI: https://doi.org/10.1039/d2py01118b
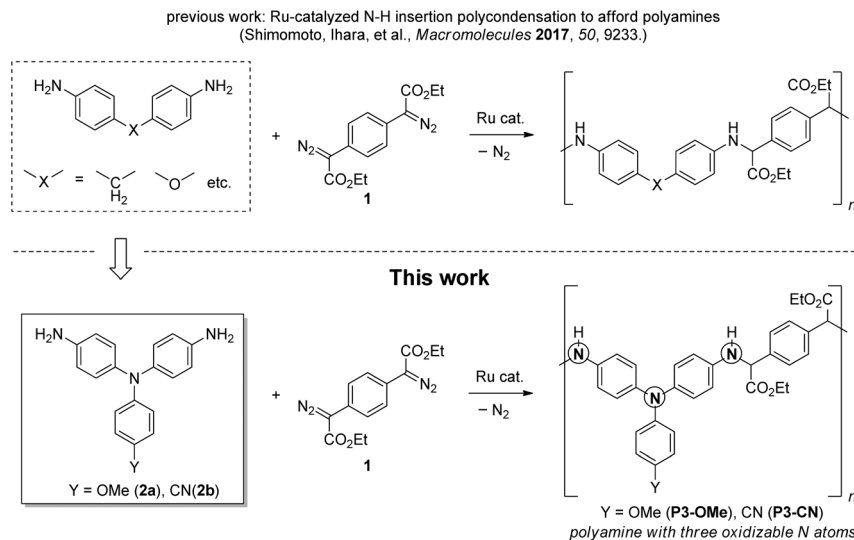
Scheme 1 Previous and this work on N−H insertion polycondensation.

2b as a diamine monomer, the resulting polyamines could have unique electroactive properties because of the presence of the diamino-TPA units in the polymer backbone;[32] in particular, it is noteworthy with the polymer structure that two nitrogen atoms originally located at the 4,4′-positions of the diamino-TPA monomers are still present as secondary amines, which can possibly participate in the electrochemical process as redox centers (Scheme 1). This feature is in sharp contrast to the previously reported TPA-based polymers such as polyimide and polyamide,[32] because in these reported examples, the nitrogen atoms originally attached to the diamino-TPA monomers were incorporated into imide or amide linkages and thus cannot participate in the redox process owing to the electron-withdrawing effect of the imide or amide carbonyl group.[33–36] Accordingly, for the diamino-TPA-bearing polyamines newly prepared in this study, it would be possible to oxidize all the three nitrogen atoms in the diamino-TPA unit in three sequential steps by gradually increasing the electrochemical potential applied to the polymer, resulting in the generation of mixed-valence (MV) systems with strong electron coupling over diamino-TPA conjugation, where the electrons can be delocalized over multiple redox states.[37,38] These systems are expected to show electrochromic (EC) behavior with multiple color changes finely responding to the gradual change of the applied potential.

In this paper, we first examined the polycondensation of diethyl 1,4-phenylenebis(diazoacetate) **1** with two types of 4,4′-diaminotriphenylamine derivatives, **2a** and **2b**, and investigated the electrochromic properties of the thin films and electrochromic devices (ECDs) of the resulting polyamines, using cyclic voltammetry (CV) and spectroelectrochemistry. As a result, we have indeed found that the presence of the secondary amino groups in the polymer backbone significantly affects the EC behavior because of the participation of the two amino groups in the redox process.

Results and discussion

Polycondensation of diethyl 1,4-phenylenebis(diazoacetate) (1) with 4,4′-diamino-4″-methoxytriphenylamine (2a) and 4,4′-diamino-4″-cyanotriphenylamine (2b)

Following the results reported in our previous publication, the polycondensation of 1,4-phenylenebis(diazoacetate) **1** with 4,4′-diamino-4″-methoxytriphenylamine **2a**[33] and 4,4′-diamino-4″-cyanotriphenylamine **2b**[34] was conducted using $[RuCl_2(p\text{-cymene})]_2$ as a catalyst under the optimized conditions: in dichloroethane at 30 °C for 12 h with a feed ratio of $[\mathbf{1} + \mathbf{2}]/[Ru] = 40$ (Scheme 2). Although the number-average molecular weight (M_n) of the products **P3-OMe** and **P3-CN** was around 8000 and somewhat lower than those reported with other diamines, well-defined polyamines with expected structures were obtained in a moderate yield of around 60% (Scheme 2). The well-defined polymer structures were confirmed from their ^1H and ^{13}C NMR spectra and the elemental analysis results [see the ESI† for the data]. For example, the ^1H and ^{13}C NMR spectra of the **P3-CN** sample (M_n = 14 000, Đ = 1.42) are shown in Fig. 1 and 2, respectively, in which all the expected signals for the repeating unit structure are observed. Likewise, the structure of **P3-OMe** was identified from its NMR spectra, although the ^{13}C NMR signals for its aromatic carbons appeared as very broad ones with some overlapping; the elemental analysis results of **P3-OMe** were satisfactory for confirming the expected polymer structure (see the ESI†).

Thermal analyses using differential scanning calorimetry (DSC) and thermogravimetric analysis (TGA) revealed that T_g (glass transition temperature) and T_{d5} (5% weight loss temperature) are 129 °C and 263 °C for **P3-OMe** and 139 °C and 260 °C for **P3-CN**, respectively, indicating their sufficient stability at higher temperatures (see the ESI†) despite the relatively low M_n of the **P3-OMe** and **P3-CN** samples below 10 000. In addition, they have good solubility in common organic sol-
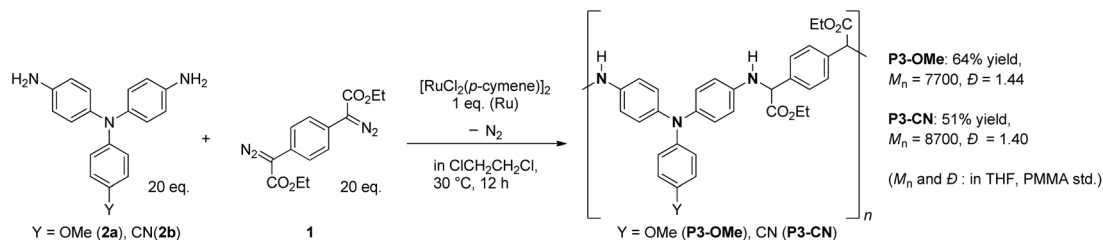
Scheme 2 Ru-catalyzed polycondensation of **1** with **2a** and **2b**.
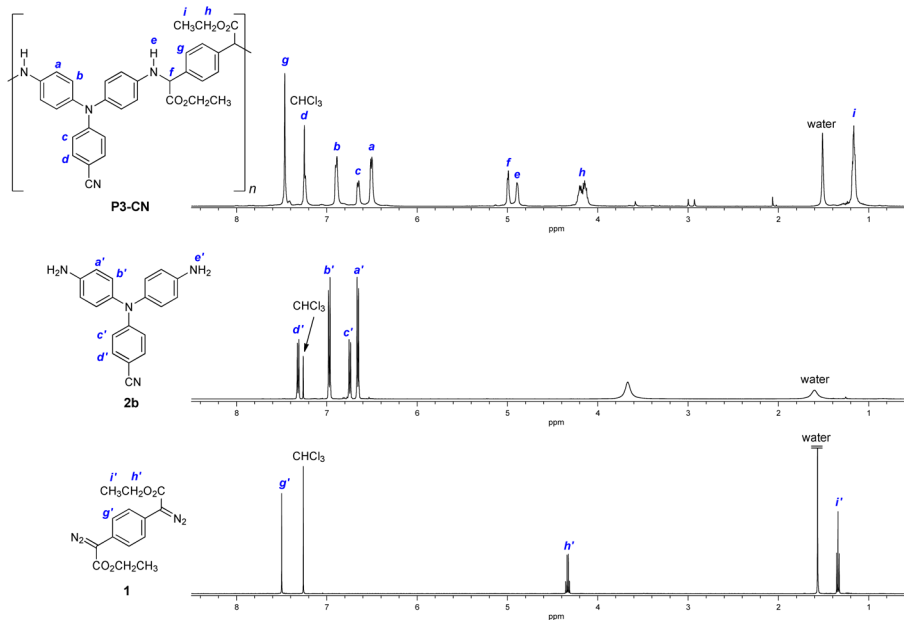
Fig. 1 ^{1}H NMR spectra of **P3-CN** (M_n = 14 000, Đ = 1.42), **2b**, and **1**.
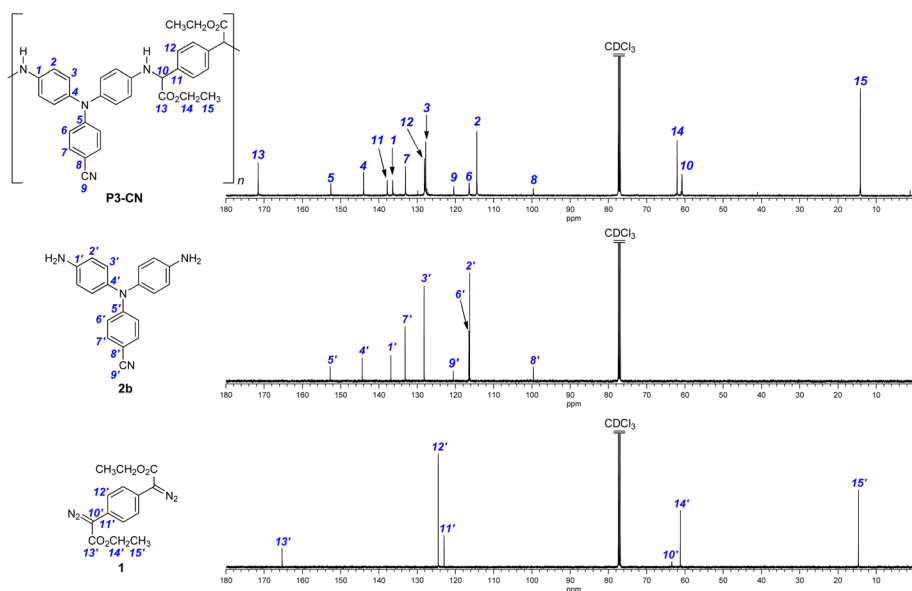
Fig. 2 ^{13}C NMR spectra of **P3-CN** (M_n = 14 000, Đ = 1.42), **2b**, and **1**.

vents such as $CHCl_3$ and THF, and their polymeric thin films can be prepared by solution cast to investigate the EC properties as shown below.

Electrochromic properties of polyamine films

Electrochemical properties. The electrochemical properties of **P3-OMe** and **P3-CN** films coated on ITO glasses were measured by cyclic voltammetry (CV) using 0.1 M $TBABF_4$ (TBA = tetrabutylammonium) as a supporting electrolyte in propylene carbonate (PC). As shown in Fig. 3(a) and (b), both **P3-OMe** and **P3-CN** films display three oxidation states in the CV diagrams, indicating that both **P3**s have three electroactive centers with different oxidation potentials derived from the presence of the three nitrogen atoms in the diamino-TPA unit. In addition, differential pulse voltammograms (DPVs) shown in Fig. 3(c) and (d) depicted three oxidation potentials for both **P3**s. Thus, the diamino-TPA unit in **P3**s should constitute a mix-valence (MV) system and lower the first stage oxidation potential, where the multiple redox states are coupled by electron delocalization over the diamino-TPA π-conjugation. This electrochemical behavior is caused by the presence of two secondary amine-nitrogen atoms directly connected to the TPA core and thus, has not been observed in the polyimide or polyamide systems obtained from the identical diamino-TPA monomers, where the corresponding nitrogen atoms cannot be electrochemically oxidized because of the electron-with-

drawing effect of the imide or amide carbonyl groups. **P3-CN** possesses higher oxidation potentials than **P3-OMe**, consistent with the substituent effect between OMe and CN previously observed in the corresponding polyamides.[33,39]

Spectroelectrochemical properties. For the **P3** films, spectroelectrochemical experiments in the visible light to near-infrared (NIR) wavelength range were conducted to evaluate the changes of the absorption spectra with increasing applied potential. The spectroelectrochemical spectra at various applied potentials of **P3-OMe** are shown in Fig. 4(a). In the neutral state (0 V), the **P3-OMe** film exhibited a strong absorption peak at 460 nm, which should be ascribed to the lowest energy π–π*-transition of the neutral diamino-TPA unit. A new strong absorption peak appeared in the NIR region at 910 nm after the first oxidation (0.4 V), suggesting that a stable monocation radical generated at the diamino-TPA center nitrogen atom electronically interacts with the remaining two neutral nitrogen atoms at the 4,4′-positions; this phenomenon is known as the intervalence charge-transfer (IV-CT) effect, which was absent in the corresponding polyamide systems because of the ineffective participation of the amide nitrogen atoms in the electrochemical process.[37] When higher potentials than 0.7 V were applied, the monocation radical structure should be transformed into a dication radical structure, making the NIR absorption band broader and hypsochromic to 840 nm with increasing intensity. In addition, a new peak at 730 nm associ-
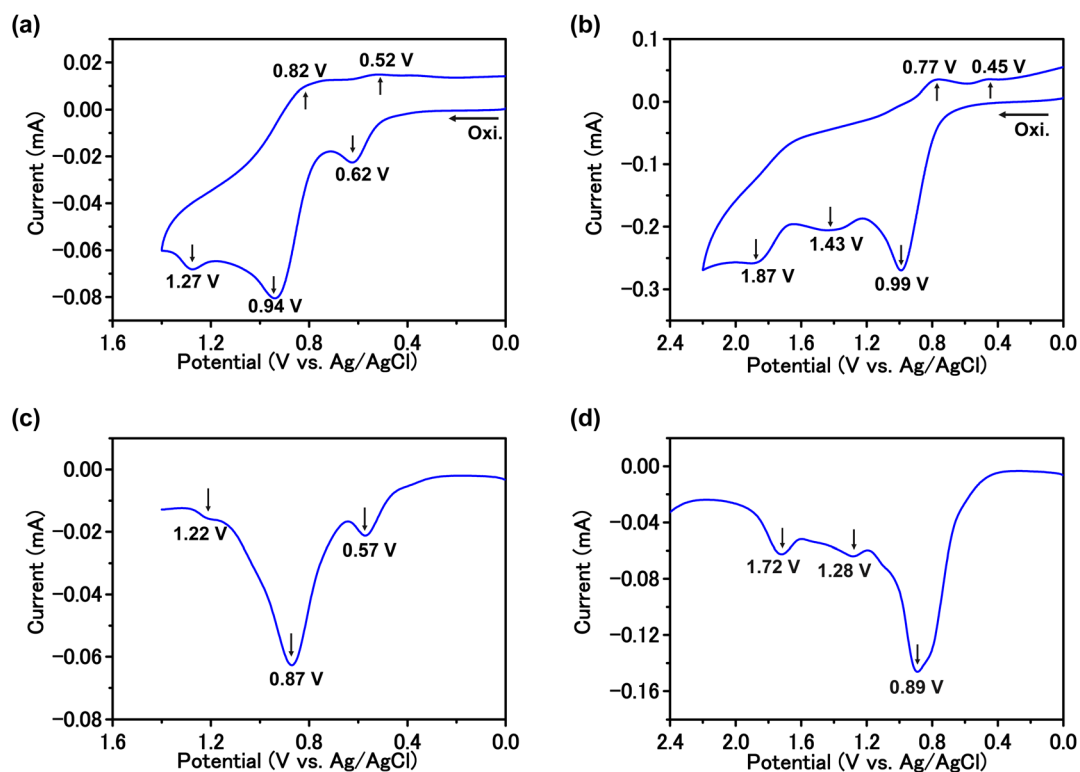

Fig. 3 Cyclic voltammetric diagrams of (a) **P3-OMe** (thickness: 500 ± 10 nm) and (b) **P3-CN** (thickness: 500 ± 40 nm) at a scan rate of 50 mV s^{-1}, and differential pulse voltammograms of (c) **P3-OMe** and (d) **P3-CN** on the ITO-coated glass substrate (coated area: 0.6 cm × 3 cm) in 0.1 M $TBABF_4$/PC.
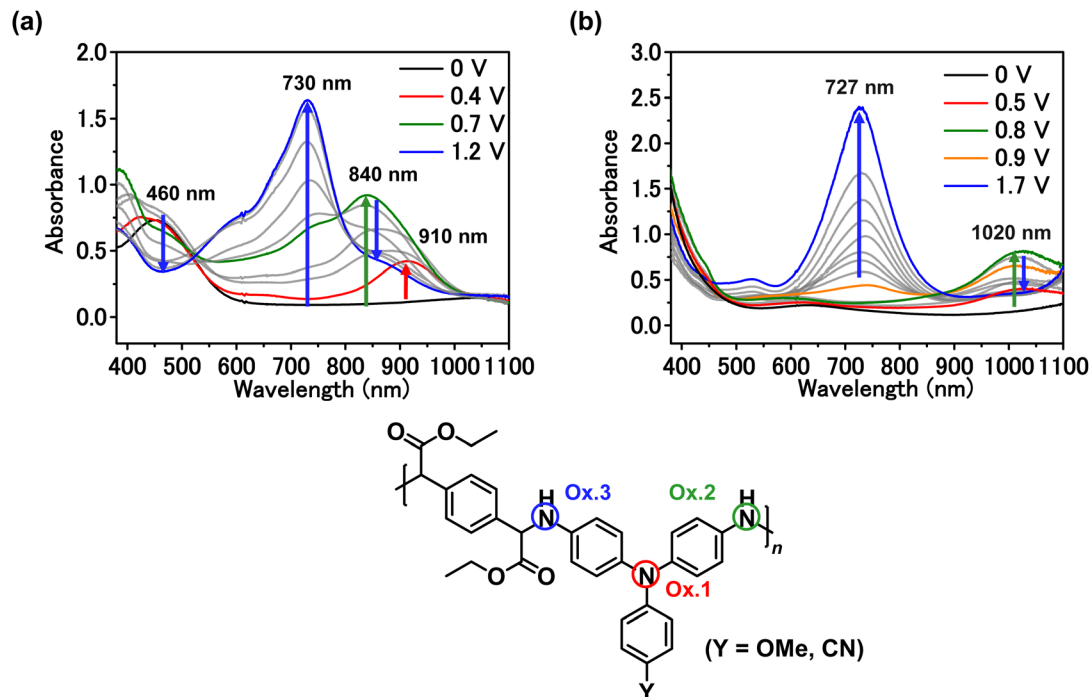
Fig. 4 Spectroelectrochemical spectra of (a) **P3-OMe** (thickness: 500 ± 10 nm) and (b) **P3-CN** (thickness: 500 ± 40 nm) in TBABF$_4$/PC at the neutral state and three oxidation states.

ated with the dication radical species was generated when the applied potential was higher than 0.4 V. These phenomena demonstrated that the formation of the oxidized secondary amine could enhance the absorbance in both the visible and NIR regions in the second oxidation state with the dication radical of diamino-TPA. Furthermore, when the potential was increased from 0.7 V to the fully oxidized state of 1.2 V, the NIR absorption band caused by IV-CT declined accordingly, indicating that the trication radical form of diamino-TPA is unfavorable for the IV-CT effect. On the other hand, the broadband peak at 730 nm gradually increased in intensity until the applied potential reached 1.2 V, suggesting that the chromophoric state causing the absorption should be present both in the di- and trication radical forms of diamino-TPA.

As depicted in Fig. 4(b), upon oxidation until the applied potential reached 0.8 V, **P3-CN** exhibited a new broad absorption peak at around 1020 nm in the NIR region due to IV-CT excitation in a similar manner to that for above-described **P3-OMe**. The significant red-shift of the absorption peak from 910 (**P3-OMe**) to 1020 (**P3-CN**) nm could be attributed to the extended π-conjugation of the monocation radical of **P3-CN** with the CN group. By increasing the applied potential to 0.9 V, the IV-CT absorption band of the cation radical started decreasing with the emergence of a new absorption peak at 727 nm owing to the beginning of the formation of a dication radical form of diamino-TPA as that observed for **P3-OMe**. As the applied potential was further increased to the third oxidation state (1.7 V), the intensity of the absorption peak at

727 nm was significantly enhanced with the disappearance of the NIR absorption band.

In accordance with the changes of the spectra with increasing potential, the darkening of the film appearance was observed despite relatively weak contrast changes (see the ESI†). It is worth mentioning that the secondary amines in the main chain of **P3**s could indeed participate in the oxidation process, in contrast to the corresponding TPA-containing polyimides and polyamides, and this feature of the new polyamine framework can be utilized for the development of highly effective EC devices.

Optical properties. The optical properties of **P3**s were investigated by UV-vis and photoluminescence (PL) spectroscopy. The results are illustrated and summarized in Fig. 5 and Table 1. **P3-OMe** and **P3-CN** exhibited maximum UV-vis absorption caused by the π–π* transitions of TPA chromophores at 306 and 290 nm in DMAc solution and 305 and 294 nm in the film state, respectively. Although the PL peak of **P3-CN** in the film state was noticeable, the intensity of 8×10^3 was much lower when compared with that of quinine sulfate in sulfuric solution ($\sim 8 \times 10^6$). Besides, according to the photoluminescence quantum yield (PLQY) measurement, the polymers **P3-OMe** and **P3-CN** in the solution or film state exhibited low (<0.5%) and non-detectable values, respectively.

Electrochromic properties of the electrochromic devices (ECDs). For further applications, ECDs were fabricated from the **P3-OMe** and **P3-CN** films with gel-type electrolyte systems using 0.015 M heptyl viologen (HV) as a cathodic EC material and 0.1 M TBABF$_4$/PC as a supporting electrolyte. During the
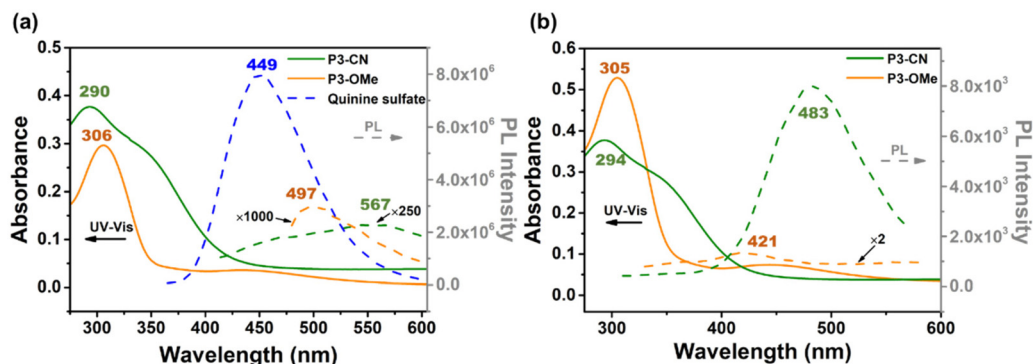
Fig. 5 UV-vis and PL spectra of polyamines (a) in DMAc solution (1 μM) and (b) in the solid state (film).

Table 1 Optical properties of the polyamines

Polyamines	DMAc solution (10 μM)			Film		
	λ_{abs} (nm)	$\lambda_{em}{}^a$ (nm)	$\Phi_{PL}{}^b$ (%)	λ_{abs} (nm)	$\lambda_{em}{}^a$ (nm)	$\Phi_{PL}{}^c$ (%)
P3-OMe	306	497	0.36	305	421	N.D.^{d}
P3-CN	290	567	0.16	294	483	N.D.^{d}

^{a} λ_{em} was excited at λ_{abs}. ^{b} The quantum yield was measured by using quinine sulfate (dissolved in 1 N H_2SO_4 at a concentration of 10 μM, assuming that the photoluminescence quantum efficiency was 0.546) as a standard at 25 °C. ^{c} PL quantum yields of the polyamine thin films were determined using a calibrated integrating sphere. ^{d} Not detected.

redox process of the ECD system, HV^{2+} could accept the electron from the diamino-TPA moiety in the oxidation process. Then, HV^+ could return the electrons to the cation radical of diamino-TPA during the reduction process. Thus, the reversible redox between HV^{2+} and HV^+ can facilitate the electron transfer between the **P3** films and the electrode, resulting in a lower oxidation potential and enhanced redox stability in the EC system, as reported in a previous study.[32,40–42]

The ECD prepared with **P3-OMe** displayed three oxidation stages in the CV diagrams, consistent with the results for the corresponding film in the absence of HV [Fig. 6(a)]. Even though the apparent oxidation potentials (0.78, 1.10, 1.73 V) are higher than those observed with the **P3-OMe** film alone (0.62, 0.94, 1.27 V) without HV as shown in Fig. 3(a), the oxidation process in the ECD occurred more efficiently considering that the electrodes employed are different in these two systems (ITO-coated glass in the ECD vs. Ag/AgCl in the film alone). As for the ECD system with **P3-CN** as shown in Fig. 6(b), because the highest applicable potential for the ECD is 2.0 V and the third oxidation potential of **P3-CN** exceeds the limitation, only two-stage oxidation was observed within this limit at apparently higher potentials (1.16 and 1.52 V) than those of the **P3-CN** film alone (0.99 and 1.43 V) as well [Fig. 3(b)].

The more efficient oxidation in the ECD systems is also observable from the CV curves in Fig. 3 and 6: in contrast to the irregular oxidation peak intensities shown in Fig. 3 [2nd oxidation peak shown in Fig. 3(a) and 1st oxidation peak shown in Fig. 3(b) are much bigger than the other oxidation peaks], the oxidation peak intensities shown in Fig. 6(a) and (b) are relatively proportional.

As illustrated in Fig. 7, the spectroelectrochemical spectra of **P3**s/HV ECDs reveal a similar optical absorption to that of **P3** films shown in Fig. 4, except that the spectra of ECDs
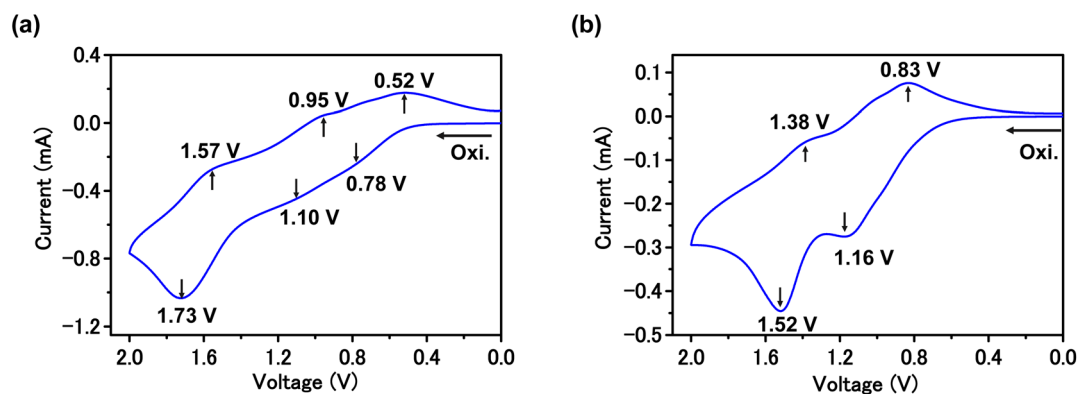

Fig. 6 Cyclic voltammetric diagrams of (a) **P3-OMe**/HV ECDs (thickness: 310 ± 30 nm) and (b) **P3-CN**/HV ECDs (thickness: 400 ± 40 nm) at a scan rate of 50 mV s^{-1} with 0.1 M TBABF$_4$ and 0.015 M HV in 0.048 mL of PC.
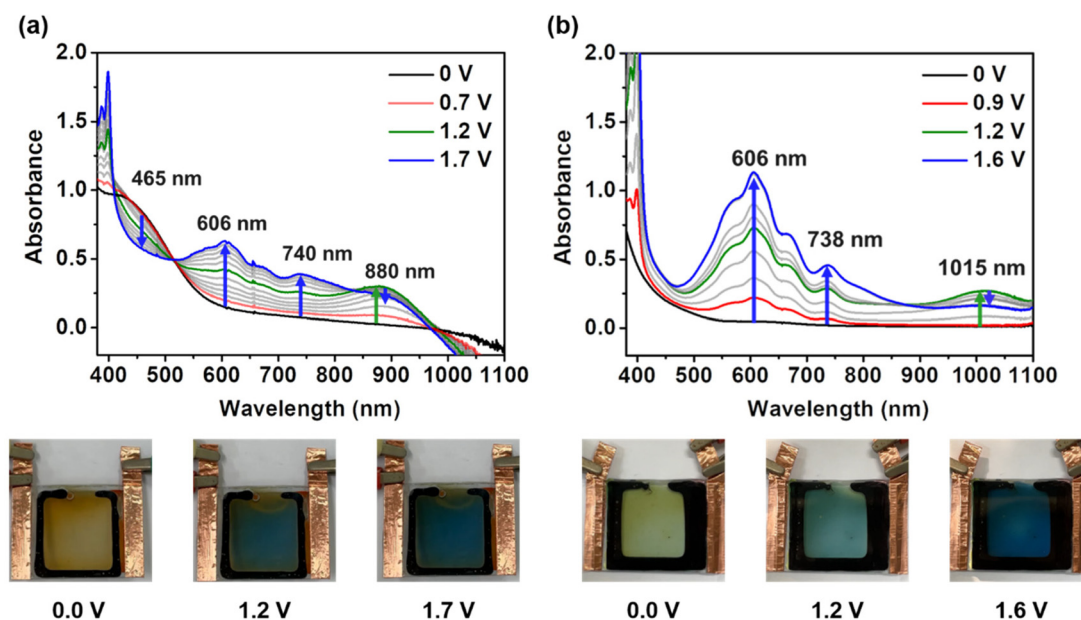
Fig. 7 Spectroelectrochemical spectrum of (a) **P3-OMe**/HV ECDs (thickness: 310 ± 30 nm) and (b) **P3-CN**/HV ECDs (thickness: 400 ± 40 nm) with 0.1 M TBABF$_4$ and 0.015 M HV in 0.048 mL of PC.

exhibit an additional HV$^+$ absorption peak at 606 nm during oxidation with the conversion of HV^{2+} to HV$^+$. The changes in the absorption spectra were consistent with the oxidation states observed in the CV diagram for the **P3**-based ECDs as shown in Fig. 6. Indeed, for both **P3** films, with the applied potential higher than 1.2 V, there was an absorption drop in the NIR region with the increased absorbance at 740 and 738 nm, indicating that for the ECDs as well, the IV-CT absorption at the NIR region decreased with increasing concentration of the trication radical form of the diamino-TPA units in the **P3** films. The **P3-OMe** ECD revealed light blue appearance at the first oxidation and became denser blue at the second oxidation state because of the increased absorption at 606 and 740 nm and decreased adsorption at 465 nm. Besides, the **P3-CN** ECD showed much lower absorption in the 400–500 nm range than the **P3-OMe** ECD and exhibited a cyan-blue color in the first oxidation state. Upon applying a potential to the second oxidation state, the color changed to dense blue because the absorption at 606 nm became dominant.

Conclusions

We have demonstrated that polyamines containing the 4,4′-diaminotriphenylamine-*N,N′*-diyl unit in the polymer backbone can be prepared by Ru-catalyzed N–H insertion polycondensation of 1,4-phenylenebis(diazoacetate) with 4,4′-diaminotriphenylamine derivatives, and that the three amino groups in the resulting polyamines are able to participate independently in the electrochemical process as redox centers with applied electrochemical potentials. The observed three-stage redox process of the new polyamines will be effective for fine-tuning

their electrochromic behavior with the applied potential. Thus, the N–H insertion polycondensation reported in this study has a distinct advantage compared to the previously reported polycondensation using 4,4′-diaminotriphenylamine derivatives as monomers affording polyimides or polyamides. This advantage will be utilized for the development of new polymeric materials for EC devices.

Conflicts of interest

There are no conflicts of interest to declare.

Acknowledgements

References

1 E. Ihara, *Adv. Polym. Sci.*, 2010, **231**, 191–231.
2 E. Jellema, A. L. Jongerius, J. N. H. Reek and B. de Bruin, *Chem. Soc. Rev.*, 2010, **39**, 1706–1723.
3 N. M. G. Franssen, A. J. C. Walters, J. N. H. Reek and B. de Bruin, *Catal. Sci. Technol.*, 2011, **1**, 153–165.

4 C. R. Cahoon and C. W. Bielawski, *Coord. Chem. Rev.*, 2018, **374**, 261–278.

5 E. Ihara and H. Shimomoto, *Polymer*, 2019, **174**, 234–258.

6 H. Shimomoto, *Polym. J.*, 2020, **52**, 269–277.

7 D. S. Tromp, M. Lankelma, H. de Valk, E. de Josselin de Jong and B. de Bruin, *Macromolecules*, 2018, **51**, 7248–7256.

8 J.-H. Chu, X.-H. Xu, S.-M. Kang, N. Liu and Z.-Q. Wu, *J. Am. Chem. Soc.*, 2018, **140**, 17773–17781.

9 N.-N. Li, X.-L. Li, L. Xu, N. Liu and Z.-Q. Wu, *Macromolecules*, 2019, **52**, 7260–7266.

10 M.-Q. Wang, H. Zou, W.-B. Liu, N. Liu and Z.-Q. Wu, *ACS Macro Lett.*, 2022, **11**, 179–185.

11 B.-R. Gao, Y.-J. Wu, L. Xu, H. Zou, L. Zhou, N. Liu and Z.-Q. Wu, *ACS Macro Lett.*, 2022, **11**, 785–791.

12 L. Zhou, L. Xu, X. Song, S.-M. Kang, N. Liu and Z.-Q. Wu, *Nat. Commun.*, 2022, **13**, 811.

13 A. V. Zhukhovitskiy, I. J. Kobylianskii, A. A. Thomas, A. M. Evans, C. P. Delaney, N. C. Flanders, S. E. Denmark, W. R. Dichtel and F. D. Toste, *J. Am. Chem. Soc.*, 2019, **141**, 6473–6478.

14 H. Shimomoto, S. Ichihara, H. Hayashi, T. Itoh and E. Ihara, *Macromolecules*, 2019, **52**, 6976–6987.

15 H. Shimomoto, R. Hohsaki, D. Hiramatsu, T. Itoh and E. Ihara, *Macromolecules*, 2020, **53**, 6369–6379.

16 H. Shimomoto, H. Hayashi, K. Aramasu, T. Itoh and E. Ihara, *Macromolecules*, 2022, **55**, 5985–5996.

17 X.-Q. Yao, Y.-S. Wang and J. Wang, *Macromolecules*, 2021, **54**, 10914–10922.

18 M. Imoto and T. Nakaya, *J. Macromol. Sci., Polym. Rev.*, 1972, **7**, 1–48.

19 E. Ihara, K. Saiki, Y. Goto, T. Itoh and K. Inoue, *Macromolecules*, 2010, **43**, 4589–4598.

20 E. Ihara, Y. Hara, T. Itoh and K. Inoue, *Macromolecules*, 2011, **44**, 5955–5960.

21 H. Shimomoto, Y. Hara, T. Itoh and E. Ihara, *Macromolecules*, 2013, **46**, 5483–5487.

22 L. Xiao, Y. Li, L. Liao and L. Liu, *New J. Chem.*, 2013, **37**, 1874–1877.

23 H. Shimomoto, H. Mukai, H. Bekku, T. Itoh and E. Ihara, *Macromolecules*, 2017, **50**, 9233–9238.

24 H. Shimomoto, T. Mori, T. Itoh and E. Ihara, *Macromolecules*, 2019, **52**, 5761–5768.

25 H. Shimomoto, T. Moriya, T. Mori, T. Itoh, S. Kanehashi, K. Ogino and E. Ihara, *ACS Omega*, 2020, **5**, 4787–4797.

26 X. Wang, Y. Ding, Y. Tao, Z. Wang, Z. Wang and J. Yan, *Polym. Chem.*, 2020, **11**, 1708–1712.

27 Z. Fu, Q. Zhou, Y. Xiao and J. Wang, *Polym. Chem.*, 2022, **13**, 2123–2131.

28 X.-Y. Zhai, X.-Q. Wang, B. Wu and Y.-G. Zhou, *Chin. J. Chem.*, 2022, **40**, 21–27.

29 L. Yin, Z. Wang, Q. Wu, L. Liu, N. Zhang, Z. Xie and G. Zhu, *ACS Nano*, 2022, **16**, 6197–6205.

30 M. Ji, S. Zheng, C. Zou and M. Chen, *Polym. Chem.*, 2022, **13**, 4782–4788.

31 Y. Xiao, Q. Zhou, Z. Fu, L. Yu and J. Wang, *Macromolecules*, 2022, **55**, 2424–2432.

32 H.-J. Yen and G.-S. Liou, *Prog. Polym. Sci.*, 2019, **89**, 250–287.

33 C.-W. Chang, G.-S. Liou and S.-H. Hsiao, *J. Mater. Chem.*, 2007, **17**, 1007–1015.

34 H.-J. Yen, C.-J. Chen and G.-S. Liou, *Chem. Commun.*, 2013, **49**, 630–632.

35 Y. Ma, Y. Hou, Y. Zhang, L. Chang, R. Li and H. Niu, *J. Appl. Polym. Sci.*, 2022, **139**, 52348.

36 X. Lv, D. Li, Y. Ma, J. Li, Y. Liu, J. Guo, H. Niu, T. Zhou and W. Wang, *Polym. Chem.*, 2022, **13**, 808–818.

37 H.-J. Yen, S.-M. Guo, G.-S. Liou, J.-C. Chung, Y.-C. Liu, Y.-F. Lu and Y.-Z. Zeng, *J. Polym. Sci., Part A: Polym. Chem.*, 2011, **49**, 3805–3816.

38 S.-H. Hsiao, G.-S. Liou, Y.-C. Kung and H.-J. Yen, *Macromolecules*, 2008, **41**, 2800–2808.

39 H.-J. Yen and G.-S. Liou, *Chem. Commun.*, 2013, **49**, 9797–9799.

40 H.-S. Liu, B.-C. Pan, D.-C. Huang, Y.-R. Kung, C.-M. Leu and G.-S. Liou, *NPG Asia Mater.*, 2017, **9**, e388.

41 J.-T. Wu and G.-S. Liou, *Chem. Commun.*, 2018, **54**, 2619–2622.

42 Y.-W. Chiu, M.-H. Pai and G.-S. Liou, *ACS Appl. Mater. Interfaces*, 2020, **12**, 35273–35281.